
TWO DIMENSIONAL NON NEWTONIAN BOUNDARY LAYER FLOW OVER A FLAT PLATE WITH POWER LAW FLUID WITH SUCTION/INJECTION THROUGH POROUS MEDIA

BALBHEEM SAIBANNA*

Research Scholar, Department of Mathematics, Central College Campus Bangalore University, Bengaluru-560001, India, Karanataka

Abstract

Keywords:

Boundary-layer equations;
Falkner-Skan equation;
Numerical solution;
porous media;
Non-Newtonian fluid;
power-law fluid;

The present paper we give numerical solution of the Falkner-Skan equation for the study of two-dimensional permeable steady boundary-layer viscous flow over a flat plate in the presence of non-Newtonian power law fluid which is represented by a power law model. The outer free stream velocity is defined in the form of a power-law manner i.e., it varies as a power of a distance from the leading boundary-layer. Generalized similarity transformations are used to convert the the governing boundary layer equations in to a third order nonlinear differential equation which is famous Falkner- Skan equation for non-Newtonian fluid. This equation contains three flow parameters that is the Stream-wise pressure gradient (β), the porous parameter (Ω), and (m) is the power law relation parrameter. The governing equations (nonlinear partial differential equations) have been converted to an equivalent nonlinear ordinary differential equation along with boundary conditions by means of which is solved using the Keller-box method. The results are obtained for velocity profiles, viscosity profiles and skin friction for various values of physical parameters and are discussed in detail. It is also found that the drag force is reduced for dilatant fluids compared to pseudo-plastic fluids. The Physical significance of the flow parameters are also discussed in detail.

Copyright © 2018 International Journals of Multidisciplinary Research Academy. All rights reserved.

Author correspondence:

First Author,
Balbheem Saibanna
Reserch Schloar, Department of Mathematics,
Central College Campus, Bangalore University,
Bengaluru-560001, India

* Doctorate Program, Linguistics Program Studies, Udayana University Denpasar, Bali-Indonesia (9 pt)

1. Introduction

The study of the boundary-layer flow of the Newtonian and non-Newtonian fluids provides valuable insights into industrial and technological applications. The Newtonian fluids such as air or water serve as a benchmark for most of the fluid flow behaviour. However the behaviour of non-Newtonian fluids that are found many industrial applications is markedly different from those of the Newtonian fluids. Particulate slurries, coal in water, sewage sludge, inks and also multiphase mixtures i.e. oil-water emulsions, foams, gas-liquid dispersions are classified as non-Newtonian fluids. Generally, these fluids have the property of a variable viscosity. One class of material of considerable interest is that the effective viscosity depends entirely on the rate of shearing on the total flow rate. For example the most commonly used models for the variable viscosity are Ostwald-de Waele, Carreau rheological fluid, Carreau-Yasuda, etc which form a relationship between shear-stress and shear ratio. Because of such applications Acrivos et al (1960) and Schowalter (1960) have obtained equations for the boundary layer flow of a non-Newtonian fluid particularly the numerical simulations of Acrivos et al (1960) show that thickness of the boundary-layer for the shear-thinning fluids is rather large compared to the shear-thickening fluids. It is further shown by Wu and Thomson (1996) that for moderate values of the Reynolds number, the boundary-layer equations for shear-thinning fluids provide accurate solutions. However, it is common practice that the boundary-layer forms when the Reynolds number is quite large.

For shear-thickening fluids, Andersson and Irgens (1998) have shown that the boundary-layer equations predict finite-width of the boundary-layer. To support these results Filipus et al (2001) gave rigorous mathematical analysis that also predicts that same finite-width of the boundary-layer. On the other hand, a self-similar solution of the boundary-layer equations results into a overshoot in the velocity profiles. In a small region in the boundary-layer, these velocity profiles exceeds the velocity of the mainstream flow. Denier and Dabrowski (2004) have even shown that these are double solutions for the boundary-layer equations when a self similar form is assumed. They further showed that mode 1 solution represents forward flow while mode 2 or mode 3 solutions become increasingly oscillatory with alternatively forward and reverse regions of flows. Results of Griffiths (2017) shown that the effects of shear-thinning are to stabilize the boundary-layer flow.

In this paper, we consider the solutions of the Navier-Stokes equations under the limit of large-Reynolds number flow that exhibiting a power-law rheological model. Among the many possible non-Newtonian fluids we have chosen the Ostwald-de Waele fluid which has a sound theoretical basis represents the complex viscosity and also it is often adopted to describe the rheological phenomena of the pseudo plastic fluids. [The boundary-layer equations admit the self-similar solutions since the mainstream flow outside the boundary-layer is approximated in power of the distance along the wedge wall.]. To solve the transformed boundary-layer equation numerically, we use the Keller-box method which is second-order accurate (Keller 1971) is used for full non-linear problem. This enables us to precisely identify the behaviour of the boundary-layer flow of the Ostwald-de Waele fluid.

Rest of the paper is organized as follows. In section 2, we set-up the problem in question in which the Cauchy momentum equations for non-Newtonian fluid. These reduce to the boundary-layer equations with inclusion of a non-linear term in the equation which models the viscosity variations. The appropriate similarity transformations are also presented. Section 3 devotes the full numerical solution of the problem. Details of numerical Keller-box method are also presented. Final section presents important findings of the problem. Here we discuss all significant results for shear-thinning and shear-thickening fluids in terms the velocity and viscosity shapes. Interestingly, the governing equation exhibits solutions for some parameter ranges.

2 Formulation of the problem

We consider the two dimensional laminar boundary-layer flow of a viscous and incompressible fluid over a flat plate through porous media with a non-Newtonian power-law fluid. The positive x -coordinate is measured along the surface and the positive y coordinate is measured normal to the x -axis in the outward direction towards the fluid. The fundamental equations for the flow of an incompressible fluid are the conservation of mass, linear momentum. We express these equations in the absence of body forces as follows

$$\nabla \cdot \vec{q} = 0 \quad (1)$$

$$\rho \left(\frac{\partial}{\partial t} + \vec{q} \cdot \nabla \right) \vec{q} = -\nabla p + \nabla \cdot \tau - kp \quad (2)$$

where ρ is the fluid density, p is the pressure, k is the permeability of the porous medium and τ is the deviatoric stress tensor and is defined as

$$\tau = \mu(\dot{q}) \quad (3)$$

where \dot{q} is the second invariant of the strain-rate tensor. The shear rate \dot{q} is given by

$$\dot{q} = \frac{1}{2} (\dot{\mathbf{q}} : \dot{\mathbf{q}})^{\frac{1}{2}} \quad (4)$$

with

$$\dot{\mathbf{q}} = (\nabla \vec{u} + \nabla \vec{u}^T) \quad (5)$$

The constitutive viscosity relation μ for the Ostwald-de Waele power-law model is given by

$$\mu = K(\dot{q})^m \quad (6)$$

where K is the material constant and the index m represents the degree of shear thickening or thinning. We note that the Newtonian viscosity relationship is recovered for $m = 1$. This parameter m is an important index which subdivides the fluids into pseudo-plastic fluids or shear-thickening when $m > 1$ and dilatants or shear-thinning for $m < 1$. Bird et al (1987) can be referred to the through account of the rheological data on m . The hydrodynamics of other values of m shall be discussed later. The velocity vector $\dot{q} = (u, v)$ where u and v are the velocity components in x and y directions respectively, and thus from (4), we have that

$$\dot{q} = \left[\left[\frac{\partial u}{\partial y} + \frac{\partial v}{\partial x} \right]^2 + \left(\frac{\partial u}{\partial x} \right)^2 + \left(\frac{\partial v}{\partial y} \right)^2 \right]^{\frac{1}{2}} \quad (7)$$

using (5). We consider the problem of two-dimensional, incompressible and steady state laminar boundary-layer flow over a wedge which moves with velocity $U_{0w}(x)$ in a non-Newtonian power-law fluid. The positive x -coordinate is measured along the surface of the wedge with the apex as origin, and the positive y -coordinate is measured normal to the x -axis in the outward direction towards the fluid. Under these approximations, the governing equations for the steady two-dimensional laminar viscous flow of a non-Newtonian fluid. It is considered that the wedge moves with velocity $U_w(x)$ along or opposite to the mainstream flows $U(x)$. Using the standard

boundary-layer approximations and for large Re we have that $\left| \frac{\partial u}{\partial y} \right| \gg \left| \frac{\partial u}{\partial x} \right|$ and $\left| \frac{\partial p}{\partial y} \right| \ll \left| \frac{\partial p}{\partial x} \right|$. Thus

the system (1)-(2) can be written as

$$\frac{\partial u}{\partial x} + \frac{\partial v}{\partial y} = 0 \quad (8)$$

$$\frac{\partial u}{\partial t} + u \frac{\partial u}{\partial x} + v \frac{\partial u}{\partial y} = -\frac{1}{\rho} \frac{dp}{dx} + \frac{K}{\rho} \frac{\partial}{\partial y} \left(\frac{\partial u}{\partial y} \right)^m - kp \quad (9)$$

Similarly, we get

$$\frac{\partial v}{\partial t} + u \frac{\partial v}{\partial x} + v \frac{\partial v}{\partial y} = -\frac{1}{\rho} \frac{dp}{dy} + \frac{K}{\rho} \frac{\partial}{\partial x} \left(\frac{\partial u}{\partial y} \right)^m - kp \quad (10)$$

where

$$\dot{q} = \frac{\partial u}{\partial y} \quad (11)$$

To this end, we consider the two-dimensional incompressible flow of the non-Newtonian Ostwald-de Waele power-law fluid over a moving wedge which is moving with velocity U_{0w} either along the mainstream flow with U_0 or opposite to it. The Cartesian coordinate system is adopted to the wedge wall the inviscid main stream velocity U_0 is assumed in the form of power of a distance that is

$$U_0(x) = U_{\infty} x^{*n} \quad (12)$$

where U_{∞} is a non-negative constant and n is a constant related to the pressure gradient defined later in this section. Now, in order to derive boundary layer conditions, the physical quantities and variables specified in (1) and (2) are non-dimensionalized

$$x = \frac{x^*}{L}, y = \frac{y^*}{\delta}, u = \frac{u^*}{U}, v = \frac{v^*}{U}, p = \frac{P^*}{P_{\infty}} \quad (13)$$

L, δ, U and P_{∞} are certain reference values. These choices lead to define the Reynolds number for the Ostwald-de Waele power-law fluid as

$$Re = \frac{\rho \delta^n U^{2-n}}{K \nu}$$

Where ν is the kinematic viscosity, for a large Re the flow divides in to near-field (boundary-layer region) and far field regions In the boundary-layer region of thickness of δ , a very large velocity gradient exists. The boundary layer equations can be derived based on the approximations concern the following measurements. Let $U_0(x)$ be the velocity of the mainstream flow along x -direction outside the boundary layer. The key idea involved in making the boundary layer approximation is that the viscosity effects are dominant in the adjacent to the surface. If δ is the thickness of the boundary layer, then $\delta \ll L$. Hence V is much smaller than U . Also other basic

approximation is $\left| \frac{\partial u}{\partial y} \right| \gg \left| \frac{\partial u}{\partial x} \right|$. Further, it is also assumed that

$\left| \frac{\partial p}{\partial y} \right| \ll \left| \frac{\partial p}{\partial x} \right|$ in meaning that the pressure p in the boundary layer is a function of x only (to the

approximation). With $\delta \ll L$ the term $\frac{\partial^2 u}{\partial x^2}$ can be neglected in comparison with $\frac{\partial^2 u}{\partial y^2}$. Velocity

compared to the free stream velocity U_∞ with these assumptions, we have the number of component equations reduce to those in the flow directions. The number of viscous terms in the direction of flow can be reduced to only dominant term. This amounts viscous terms are measured in terms of the boundary-layer thickness. And the inertial terms of the characteristic length L . Thus along with these boundary- layer approximations. Equations (8), (9) and (10) for steady case may be written as

$$\frac{\partial u}{\partial x} + \frac{\partial v}{\partial y} = 0, \quad (14)$$

$$u \frac{\partial u}{\partial x} + v \frac{\partial u}{\partial y} = -\frac{1}{\rho} \frac{dp}{dx} + \frac{K}{\rho} \frac{\partial}{\partial y} \left(\frac{\partial u}{\partial y} \right)^m - \frac{v}{k} (u - U) \quad (15)$$

$$0 = \frac{\partial p}{\partial y} \quad (16)$$

where K is called the consistency coefficient and m is non-dimensional, and the dimension of K depends on the value of m . The two-parameter rheological equation (15) is known as the Ostwald-de-Waele model or more commonly, the power-law model. The parameter m is an important index to subdivide fluids into pseudo-plastic fluids ($m < 1$) and dilatant fluids ($m > 1$). The extreme cases of the power-law model are ($m = 1$) for Newtonian behaviour and ($m = 0$) for plastic or solid behaviour. To determine the pressure distribution, the velocity at the edge of the boundary layer is equal to the mainstream flow $U_0(x)$ and by Bernoulli's theorem, the pressure would be constant in the inviscid flow influenced by the applied magnetic field. In order that equations (14) and (15) reduce to similarity form, we assume that the boundary conditions for these equations are of the following form

$$\text{at } y = 0 : u = 0, v = V_w(x)$$

$$\text{as } y \rightarrow \infty : u \rightarrow U_{0\infty} \quad (17)$$

where $U_0 w(x)$ is the stretching surface velocity which obeys the power-law relation $U_0 w(x) = U_{0\infty} x^m$. The conditions on the velocity at infinity mean that the velocity approaches the mainstream flow far-away from the wedge surface. Thus, the main boundary layer effects are restricted to the immediate neighbourhood of the surface. System (14) and (15) allows reducing both dependent and independent variables to one each by the following similarity transformations. This is further evidenced by the similar velocity profiles existing in the boundary layer for any x in the stream wise direction. The pressure change across the boundary layer is negligible (i.e., constant) and pressure can be treated as function of only flow direction.

Since the pressure is uniform throughout the flow field from the Bernoulli's equation, with $u = U_{0\infty}$ outside the boundary layer, we have

$$-\frac{1}{\rho} \frac{dp}{dx} = U_0 \frac{dU_0}{dx} \quad (18)$$

$$u \frac{\partial u}{\partial x} + v \frac{\partial u}{\partial y} = U_0 \frac{dU_0}{dx} + \frac{K}{\rho} \frac{\partial}{\partial y} \left(\frac{\partial u}{\partial y} \right)^m - \frac{v}{k} (u - U_0(x)) \quad (19)$$

It is clearly observed that the system (14) and (15) with two unknown functions u and v are easily reduced to an equation with one unknown function by defining the stream function $\psi(x, y)$ as

$$u = \frac{\partial \psi}{\partial y} \quad \text{and} \quad v = -\frac{\partial \psi}{\partial x} \quad (20)$$

$$\frac{\partial \psi}{\partial y} \frac{\partial^2 \psi}{\partial x \partial y} + \frac{\partial \psi}{\partial x} \frac{\partial^2 \psi}{\partial y^2} = U_0(x) \frac{dU_0(x)}{dx} + \frac{K}{\rho} \frac{\partial}{\partial y} \left(\frac{\partial u}{\partial y} \right)^m - \frac{v}{k} (u - U_0(x)) \quad (21)$$

with boundary conditions

$$y = 0: \quad \frac{\partial \psi}{\partial x} = 0, \quad \frac{\partial \psi}{\partial y} = V_w(x)^n \quad \text{and as} \quad \frac{y}{\partial} \rightarrow \infty: \quad \frac{\partial \psi}{\partial y} = U_{0\infty}(x)^n \quad (22)$$

The similar solutions of equation (21) can be obtained by using similarity transformation

$$\psi(x, y) = \sqrt{\frac{2\nu K U_{0\infty} x^{1+m^*}}{\rho(n+1)}} f(\eta), \quad \eta = \sqrt{\frac{(n+1)\rho U_{0\infty} x^{-1+m^*}}{2K\nu}} y$$

(23)

$$\text{where } m^* = \frac{(3n-1)(m-1)}{m+1}$$

Substituting (23) in to (21) we get the following ordinary differential equation

$$\mu_0 f''' + \frac{2}{m+1} f f'' + \frac{\beta}{1+(m-1)\beta} (1-f'^2) - \Omega(f'-1) = 0$$

(24)

and a new set of boundary conditions,

$$f(0) = \alpha, \quad f'(0) = 0, \quad \text{and} \quad f'(\infty) = 1 \quad (25)$$

where $\mu_0(\eta) = m|f''(\eta)|^{m-1}$ where primes denote differentiation with respect to η and $\lambda = \frac{U_{0w}}{U_{0\infty}}$ is

the ratio of the wall velocity to the free stream fluid velocity. And $\beta = \frac{2n}{n+1}$ is the pressure

gradient variable parameter. The system (24)-(25) describes the two-dimensional permeable laminar boundary layer flow of a viscous fluid through porous media. Hence

$\alpha = \sqrt{\frac{2x}{(m+1)\nu U(x)}} V_w(x)$ is the suction or injection parameter $\alpha > 0$, represents suction and α

< 0 is injection, whenever $\alpha = 0$ is impermeable of the plate, $\beta > 0$ is the favorable, and $\beta < 0$ is

adverse pressure gradient where as $\Omega = \frac{2\left(\frac{U_\infty}{\nu}\right)^{(m-2)}}{k(m+1)\text{Re}^{(m-1)}}$ is the permeability. For $\beta = 0 = \Omega$, the

above problem reduce to the Blasius flow that describes a two-dimensional flow over a flat plate with mass transfer and stretch of the plate, and is studied by several investigators with different cases. The system (24)-(25) describes the flow of Ostwald-de-Waele fluid in the two-dimension boundary-layer flow. Since any analytical solution is usually not possible because of high non-linearity, we solve the system (24) and (25) numerically using the Keller-box method which is employed in most of boundary-layer simulations.

3. Numerical solution

We solve (24) with the boundary conditions (25) using Keller-box method for different values of β, m and Ω . We briefly give about two-point Keller-box method for the solution of (24). This scheme is very efficient and fast, and can be used to solve the boundary-layer problems. A detailed description about the method is given in Cebeci and Bradshaw (1977), Kudenatti et al (2013), and in the review paper given by Keller (1978). By using this method we are able to obtain approximations to the solutions of the original differential equation at each grid point. This method is unconditionally stable and has quadratic convergence even for non-uniform mesh points (Cebeci and Cousteix (1999)). To describe this method, the equation (24) with the boundary conditions (25) are rewritten in the form of system of first order ordinary differential equations and are given by

$$f' = U \tag{26}$$

$$U' = V \tag{27}$$

$$BV' + \frac{2}{m+1}fV + \frac{\beta}{1+(m-1)\beta}(1-U^2) - \Omega(U-1) = 0 \tag{28}$$

where $B = \mu_0 = m|V|^{m-1}$ and boundary conditions equation (25) becomes

$$f(0) = \alpha, U(0) = 0 \text{ and } U(\infty) = 1 \tag{29}$$

Using the backward finite difference operators for the system (26-28), we get

$$f_j^l - f_{j-1}^l - \frac{\eta_j}{2}(U_j^l - U_{j-1}^l) = 0$$

$$U_j^l - U_{j-1}^l - \frac{\eta_j}{2}(V_j^l - V_{j-1}^l) = 0$$

$$BV_j^l - BV_{j-1}^l - \frac{\eta_j}{2(m+1)}(f_j^l - f_{j-1}^l)(V_j^l - V_{j-1}^l) - \frac{\eta_j\beta}{4(1+(m-1)\beta)}(U_j^{l-1} + U_{j-1}^{l-1})^2 + \frac{2\eta_j\beta}{1+(m-1)\beta} -$$

$$\Omega \frac{\eta_j}{2}(U_j^l + U_{j-1}^l) + 2\Omega\eta_j = 0$$

The above system necessarily produces a nonlinear algebraic system of equations for each grid. We linearize the above system by introducing, $f_j^{(l+1)} = f_j^l + \delta f_j^l$, where δf_j^l has to be corrected at each step, we drop the product terms of like $\delta f_j^l, \delta V_j^l$ etc and also neglected square terms in δf_j^l , then, we get

and the boundary conditions are

$$\delta f_0 = \delta U_0 = 0, \delta U_N = 0$$

$$f_0 = \alpha, U_0 = 0, U_N = 1 \tag{30}$$

$$\delta f_j - \delta f_{j-1} - \frac{\eta_j}{2}(\delta U_j + \delta U_{j-1}) = f_{j-1} - f_j + \frac{\eta_j}{2}(U_j - U_{j-1}) \tag{31}$$

$$\delta U_j - \delta U_{j-1} - \frac{\eta_j}{2}(\delta V_j + \delta V_{j-1}) = U_{j-1} - U_j + \frac{\eta_j}{2}(V_j - V_{j-1}) \tag{32}$$

$$c_1 \delta V_j + c_2 \delta V_{j-1} + c_3 \delta f_j + c_4 \delta f_{j-1} + c_5 \delta U_j + c_6 \delta U_{j-1} =$$

$$-\frac{4d\beta}{1+(m-1)\beta} + BV_{j-1} - BV_j - \frac{d}{m+1}(f_j V_j - f_{j-1} V_{j-1}) + \frac{d\beta}{2(1+(m-1)\beta)}(U_j + U_{j-1})^2 +$$

$$\Omega \frac{\eta_j}{2}(U_j + U_{j-1}) \tag{33}$$

Where $d = \frac{\eta_j}{2}$,

$$c_1 = B + \frac{d}{m+1}(f_j + f_{j-1}), c_2 = -B + \frac{d}{m+1}(f_j + f_{j-1}), c_4 = \frac{d}{m+1}(V_j + V_{j-1})$$

$$c_5 = -\frac{d\beta}{1+(m-1)\beta}(U_j + U_{j-1}) - \Omega d, c_6 = -\frac{d\beta}{1+(m-1)\beta}(U_j + U_{j-1}) - \Omega d,$$

At $j = 1$,

from equations (31-33) we get,

$$\delta f_1 - \delta f_0 - d \delta U_1 - d \delta U_0 = f_0 - f_1 + d U_1 - d U_0$$

$$\delta U_1 - \delta U_0 - d \delta V_1 - d \delta V_0 = U_0 - U_1 + d U_1 - d U_0$$

$$c_1 \delta V_1 + c_2 \delta V_0 + c_3 \delta f_1 + c_4 \delta f_0 + c_5 \delta U_1 + c_6 \delta U_0 =$$

$$-\frac{4d\beta}{1+(m-1)\beta} + BV_0 - BV_1 - \frac{d}{m+1}(f_1 V_1 - f_0 V_0) + \frac{d\beta}{2(1+(m-1)\beta)}(U_1 + U_0)^2 +$$

$$\Omega d(U_1 + U_0) - 2d\Omega$$

Using the above boundary conditions (30) in (31) - (33) we get a block tridiagonal matrix wherein each element is again 3×3 matrix, in the form

$$AD = R \tag{35}$$

is essentially a linear system

$$A_1 = \begin{bmatrix} 0 & 1 & 0 \\ -d & 0 & -d \\ c_2 & c_3 & c_1 \end{bmatrix}, A_j = \begin{bmatrix} -d & 1 & 0 \\ -1 & 0 & -d \\ c_6 & c_3 & c_1 \end{bmatrix}$$

$$B_j = \begin{bmatrix} 0 & -1 & 0 \\ 0 & 0 & -d \\ 0 & c_4 & c_2 \end{bmatrix}, C_{j-1} = \begin{bmatrix} -d & 0 & 0 \\ 1 & 0 & 0 \\ c_5 & 0 & 0 \end{bmatrix}$$

$$D = [\delta_1, \delta_2, \dots, \delta_N]^T, \delta_j = [f, U, V]^T, R = [R_1, R_2, \dots, R_N]^T, R_j = [R_{1j}, R_{2j}, R_{3j}]^T,$$

$$\delta_1 = \begin{bmatrix} \delta V_0 \\ \delta f_1 \\ \delta V_1 \end{bmatrix}, \delta_2 = \begin{bmatrix} \delta U_1 \\ \delta f_2 \\ \delta V_2 \end{bmatrix}, \dots, \delta_N = \begin{bmatrix} \delta U_{N-1} \\ \delta f_N \\ \delta V_N \end{bmatrix}$$

where $j = 2, 3, 4, \dots$. The tridiagonal structure (35) can be solved using LU decomposition method. The velocity equation for similar for each pressure gradient and permeable parameters the Keller-box code also given other required derived quantities such as the velocity profiles. The numerical solution of equation (24) for different parameters, β, Ω , and m has been obtained. Results for the skin friction coefficient, velocity profiles and numerical solutions are reported. The drag force is reduced for dilatant fluids compared to pseudo-plastic fluids.

4 Results and Discussion

The similarity solutions of the permeable Falkner-Skan equation for non-Newtonian fluid are obtained for all physical parameters. This equation describes flow of a viscous fluid through porous media. The flow is governed by the nonlinear differential equation of order three and is solved by different approaches. The validity and efficiency of the solution method are tested for various parametric values of β, Ω and m are compared with the numerical solution of the permeability Falkner-Skan equation. We also investigated the nature of the distribution of velocity in the boundary layer region at which the effects of permeability taken into account. Numerical values for these parameters are taken which have been extensively used in the previous theoretical studies. In particular, we have taken the range of values for which the solutions are predicted and boundary layer flows are realized. Further, the direct numerical solutions of the permeability Falkner-Skan equation are obtained via finite difference based Keller-box method. This is a standard method for solving nonlinear boundary value problem on a closed interval, in which the Falkner-Skan is converted into an equivalent system of first order equations. The outer boundary condition is taken at very large value of η that is $\eta_{\max} \gg 1$. The standard central difference schemes are used for the first order equations, and resulting nonlinear algebraic equations are linearized and solved. Our Keller-box code adapts a variable discretization step size to ensure the desired accuracy in a double precision which was set to 10^{-8} in all our computations. This is because a precise value of $f''(0)$ would be required to compare solution with the numerical ones.

The values for β and m are so chosen to be in the range of parameters that have been used in the previous studies (Bird et al (1987)). Also, full numerical Keller-box results using $\Delta\eta = 0.01$ are compared with those obtained with still smaller $\Delta\eta = 0.001$ values and the velocity shapes between two are graphically matchable; thus, most of the simulations are performed with $\Delta\eta = 0.01$. Further, the value of N (the number of grid points) depends on the value $\Delta\eta$ of η and the large values of integration-domain lengths (see figures for details). We discuss most of our results pertaining to $m \neq 1$ which is regarded as a generic problem as $m = 1$ case has been fully discussed. The case $m = 1$ also serves as the bench-mark of present study.

In order to get the physical insight, numerical computations are carried out for various sets of physical parameters on skin friction coefficient, pressure gradient variable parameter β , suction or injection parameter α and permeability parameter Ω to obtain the effects of those parameters on dimensionless velocity. The obtained computational results (variations in velocity and viscosity profiles) are presented graphically in from figures 1 to 8

Figures 1 and 4 depicts that the variation of velocity profiles $f'(\eta)$ as a function of η for different values of permeability parameter. There have been simulated using the Keller-box numerical method that is described in section 3. This code starts to predict permeability effects on the boundary-layer flow. It is noticed that thickness of the boundary-layer thickness increases for increasing permeability. It is very clear that from the boundary-layer shear-thickening when $m > 1$ (i.e. in dilatant fluids) and when $m < 1$ the boundary-layer shear-thinning (i.e. in pseudo-plastic fluids) for fixed values of α, β and m . The two extreme cases of the power-law model are $m = 1$ for Newtonian behaviour and $m = 0$ for plastic or solid behaviour.

Figure 2 exhibits the nature of velocity profiles $f'(\eta)$ as a function of η . It is very clear that for fixed Ω, β and α the boundary-layer decreases as increase m . The effect of non-Newtonian parameter m for fixed values of Ω, β and α on velocity fields are depicted. When suction parameter $\alpha = 1.0$ velocity increases exponentially as decrease in m increases monotonically as decrease in m for $\alpha = -1.0$.

It is worthwhile to note from the figure 4 that, variation of viscosity profiles $\mu_o(\eta)$ with η the suction parameter $\alpha > 0$ and injection parameter $\alpha < 0$ viscosity decreases as increases m in both case when $\beta = 0.46$ and $\beta = 1.0$ for fixed values of Ω and β .

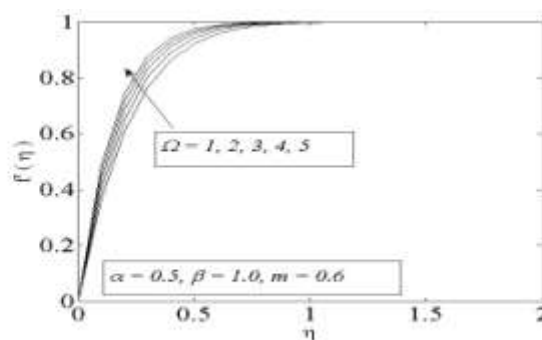


Figure 1(a): Variation of Velocity profiles $f'(\eta)$ with η for various values of Ω , $\alpha = 0.5$, $\beta = 1$, and $m = 0.6$

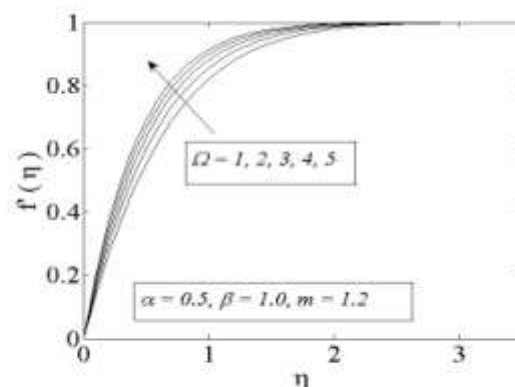


Figure 1(b): Variation of Velocity profiles $f'(\eta)$ with η for various values of Ω , $\alpha = 0.5$, $\beta = 1$, and $m = 1.2$

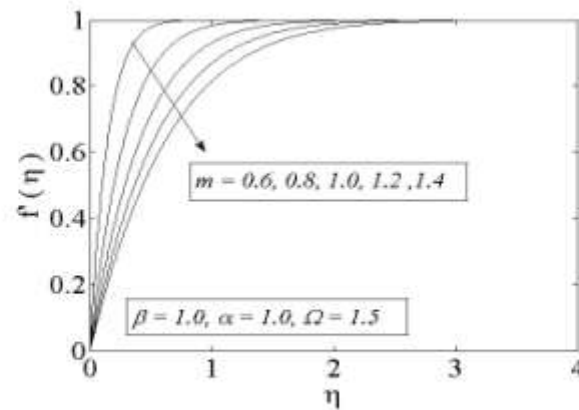


Figure 2(a): Variation of Velocity profiles $f'(\eta)$ with η for various values of m , $\alpha = 1, \beta = 1$, and $\Omega = 1.5$

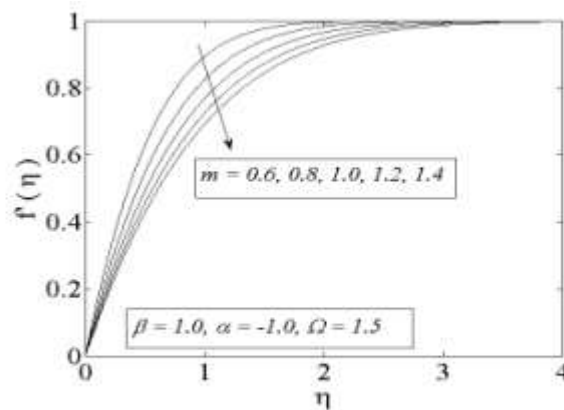


Figure 2(b): Variation of Velocity profiles $f'(\eta)$ with η for various values of m , $\alpha = -1, \beta = 1$, and $\Omega = 1.5$

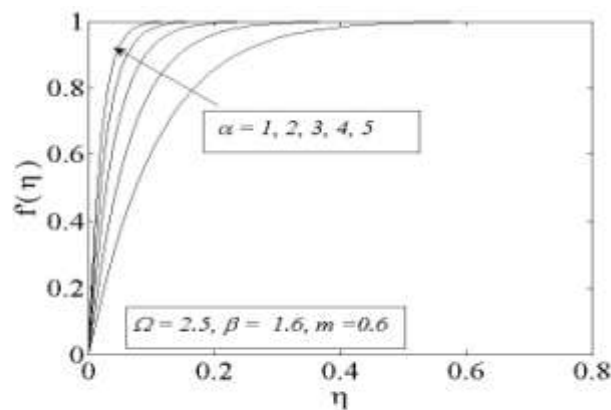


Figure 3(a): Variation of Velocity profiles $f'(\eta)$ with η for various values of α , $m = 0.6$, $\beta = 1.6$, and $\Omega = 2.5$

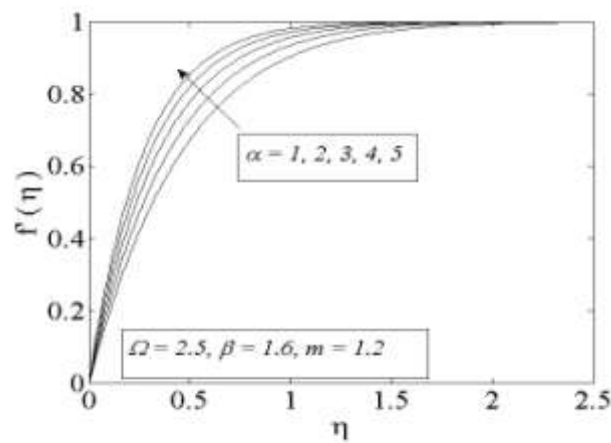


Figure 3(b): Variation of Velocity profiles $f'(\eta)$ with η for various values of α , $m = 1.2$, $\beta = 1.6$, and $\Omega = 2.5$

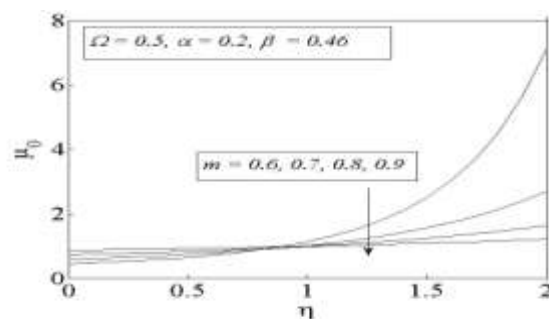


Figure 4(a): Variation of Velocity profiles μ_0 with η for various values of m , $\alpha = 0.2$, $\beta = 0.46$, and $\Omega = 0.5$

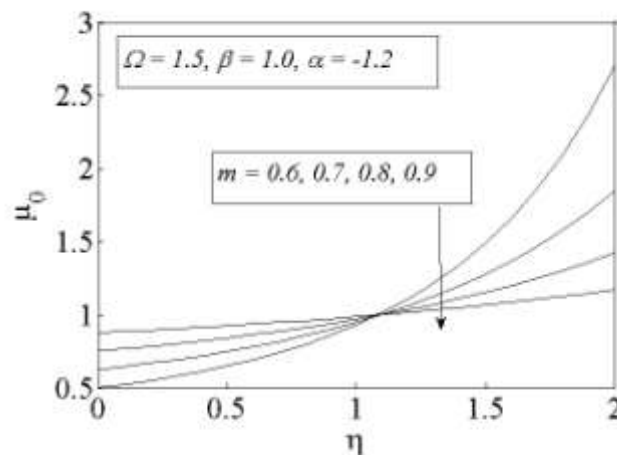


Figure 4(b): Variation of Velocity profiles μ_0 with η for various various values of m , $\alpha = -1.2$, $\beta = 1$ and $\Omega = 1.5$

REFERENCES

- 1) A. Acrivo, M.J. Shah, and E. F. Petersen, On the Flow of a Non-Newtonian Liquid on a Rotating Disk
Journal of Applied Physics **31**, 963 (1960).
- 2) W. R. Schowalter, The Application of Boundary-layer Theory to Power-Law Pseudoplastic Fluids: Similar Solutions, AIChE Journal volume 6, Issue 1, March 1960 pages 24-28.
- 3) H. I. Andersson and F. Irgens, Gravity-Driven Laminar-Film Flow Mech. 27, 153-172 (1998).
- 4) P. James Denier and P. Paul Dabrowski, On the Boundary-Layer Equations for Power-Law Fluids. Proceedings: Mathematical, Physical and Engineering Sciences Vol. 460, 2051 (Nov. 8, 2004), PP. 3143-3158.
- 5) P. T. Griffiths, Stability of the Shear-Thinning Boundary-Layer Flow Over a Flat Inclined Plate, Proceedings of the Royal Society a Mathematical, Physical and Engineering Sciences 6th September 2017.
- 6) T. Cebeci, and P. Bradshaw, Momentum Transfer in Boundary-Layers Corp: New York, McGraw-Hill Book CO, 1977, 407p.
- 7) R. B. Kudenatt, S. R. Kirsur, L. N. Achala and N. M. Bujurke, MHD Boundary-Layer Flow Over a Non-Linear Stretching Boundary with Suction and Injection, International Journal of Non-Linear Mechanics 50 (2013) 58-67.
- 8) T. Cebeci and J. Cousteix Modeling and Computation of Boundary-Layer Flows – Laminar, Turbulent and Transitional Boundary-Layers in Incompressible Flows, Long Beach, Calif.: Horizons Pub. Berlin; New York: Springer, (1999).